Available online at www.sciencedirect.com
SCIENCE DIRECT®
Journal of Solid State Chemistry 177 (2004) 3824–3829
JOURNAL OF SOLID STATE CHEMISTRY
www.elsevier.com/locate/jssc

Micro-sized Sb_2O_3 octahedra fabricated via a PEG-1000 polymer-assisted hydrothermal route

Xuchu Ma, Zude Zhang*, Xuebing Li, Yi Du, Fen Xu, Yitai Qian

Structure Research Laboratory, Department of Chemistry, The University of Science and Technology of China, Number 96, JinZhai Road, Hefei City, Anhui Province 230026, People's Republic of China

Received 18 May 2004; received in revised form 2 July 2004; accepted 2 July 2004
Available online 27 August 2004

Abstract

The micro-sized Sb_2O_3 octahedra can be synthesized on a large scale via a simple PEG-1000 polymer-assisted hydrothermal route (PAHR) in the temperature range of 160–180 °C for 10–14 h. The structures, compositions, and morphologies of the as-synthesized products are derived from X-ray power diffraction pattern, X-ray photoelectron spectra, and field emission scanning electronic microscope. Meanwhile, the optical properties of the micro-sized Sb_2O_3 octahedra are studied by their photoluminescene spectroscopy and Raman spectrum. Furthermore, the possible growth mechanism of the micro-metered Sb_2O_3 octahedra is discussed on the basis of a series of supplementary experiments. And it has been found that PEG-1000, sodium tartrate, the reaction temperature, and the reaction time have considerable effects on the final morphology of Sb_2O_3, while the pH value has an influence on the formation of the Sb_2O_3 crystals.

Keywords: Micro-octahedra; Hydrothermal crystal growth; Sb_2O_3; Polymer assisted

1. Introduction

Microchemistry encompasses many areas of chemical experimentation and may be defined as a branch of chemical science, which deals with the principles and methods for using the minimum quantity of materials to obtain the desired chemical information and applications [1–3]. For example, silver or gold microwires with diameters of ca. 1 μm, consisting of periodically varying metals with different reflectivity have been shown to be useful as barcodes in biodiagnostics [4]. In principle, the same effect of differential reflectivity could be obtained if the wire diameter varies periodically, or even non-periodically, via a controlled process [5]. Therefore, the development of not only facile but also controllable synthetic methods in the synthesis of the micro-sized materials is of significance [6].

Antimony oxide (Sb_2O_3) is useful for the flame retardant when using it together with halogen-containing resin and halogenated flame retardant. Extremely fine particles of colloidal antinomy phenoxide have wide application as optical materials because of their high refractive index and high abrasive resistance. Recently, it has been reported that hydrous antinomy oxide can exhibit high proton conductivity, which makes Sb_2O_3 extremely useful as humidity-sensing materials [7,8]. Furthermore, micro-sized Sb_2O_3 crystals are intrinsically attractive candidates for application as catalyst and fining agent, owing to the fact that micro-sized Sb_2O_3 crystallines can be expected to display better properties than coarsely grained powders. Various methods have been reported on the synthesis of Sb_2O_3 materials, such as heating antimonic acid in air [9], a γ-ray irradiation–oxidization route [10], microemulsion [11–13], vapor condensation method [14], vapor–solid route [15], surfactant-assisted solvothermal process [16], and carbon nanotubes template-assisted synthesis [17].

*Corresponding author. Fax: +86-551-360-1592.
E-mail address: zhanglab@ustc.edu (Z. Zhang).

0022-4596/$ - see front matter © 2004 Elsevier Inc. All rights reserved.
doi:10.1016/j.jssc.2004.07.005

However, there are few reports about the large-scaled growth of micro-metered Sb_2O_3 octahedra under the assistant of PEG polymers.

Can Sb_2O_3 atoms or building blocks be assembled into the perfect polyhedrons in the presence of PEG polymers? The answer is positive. Here, we report a simple PEG-1000 polymer-assisted hydrothermal route (PAHR) for the large-scaled synthesis of the micro-sized Sb_2O_3 octahedra in the temperature range of 160–180 °C for 10–14 h. Some fascinating features are described in the present work: (i) Sb_2O_3 micro-octahedra are of uniform size; (ii) the yield is as high as ~90%; and (iii) the route is very simple and controllable, which can be expected to extend to fabricate other micro-sized materials.

2. Experimental

In the typical procedure, 0.228 g (1 mmol) antimony trichloride ($SbCl_3$), 0.92 g (4 mmol) sodium tartrate ($C_4H_4O_6Na_2 \cdot 2.5H_2O$), 0.1 g (1 mmol) poly(ethylene glycol) (PEG, molecular weight = 1000), 30 mL distilled water are mixed, and the mixture is stirred for 30 min till the solution is transparent, then the final pH value of the mixture is adjusted to 9 by slowly adding an aqueous solution of NaOH (1.0 mol L^{-1}). This solution is transferred into the Teflon-lined stainless-steel autoclave of 50 mL capacity and the autoclave is maintained at 180 °C for 12 h, then allowed to naturally cool to room temperature. After washing with absolute alcohol and distilled water for several times, white precipitates are obtained and dried in vacuum at 50 °C for 3 h.

The composition of the as-prepared product is determined by X-ray powder diffraction (XRD), using a Philip X' Pert PRO SUPER rA rotation anode with Ni-filtered Cu$K\alpha$ radiation ($\lambda = 1.541874$ Å) at 25 °C. X-ray photoelectron spectroscopy (XPS) is performed on ESCALAB MKII with MgK_α ($h\nu = 1253.6$ eV) as the exciting source at a pressure of 1.0×10^{-4} Pa and a resolution of 1.00 eV. The binding energies obtained in the XPS analysis are corrected for specimen charging by referencing the C_{1s} to 284.4 eV. The overview morphologies of the crystals are observed by field electron scanning electronic microscope (FE-SEM), taken on a JEOL JSM-6700F SEM. Scanning electron microscopy (SEM) images are taken with an X-650 scanning electron microanalyzer. The photoluminescence (PL) spectra of Sb_2O_3 micro-octahedra are measured by a PELS55-luminescence spectrometer with a Xe lamp at 25 °C. Raman spectrum was recorded on a ram-HI spectrometer with the excitation wavelength of 514.5 nm and a power less than 5 mW.

3. Results and discussion

3.1. Characterization

The XRD pattern in Fig. 1 demonstrates that well-crystallized Sb_2O_3 powders can be easily obtained at 180 °C, and all the diffraction peaks can be indexed to cubic Sb_2O_3 with the cell parameters of $a = 11.13$ Å, which is in good agreement with the literatures (JCPDS Files, No. 75-1565, $a = 11.14$ Å). No other noticeable peaks induced by impurities can be observed in the XRD patterns.

The purities and the electronic binding energy of the products could be derived from the XPS spectra (shown in Fig. 2). Fig. 2a is the typical survey spectrum of the micro-sized Sb_2O_3 octahedra, indicating the presence of Sb and O elements. The appearance of C impurities peaks is due to the absorption of CO_2 on the surface of the sample. The Sb 3d spectra (shown in Fig. 2b) exhibit two slightly asymmetrical peaks containing $3d_{5/2}$ and $3d_{3/2}$, and from Fig. 2b, it can be found that the strong peaks centered at 529.79 and 539.25 eV correspond to the Sb $3d_{5/2}$ and Sb $3d_{3/2}$ binding energy, respectively, which coincides with the reported values in the literature [18]. Since the position of the Sb $3d_{5/2}$ binding energy is superposed with that of the O 2p binding energy, the Sb $3d_{3/2}$ binding energy is taken for the characterization. After deducting the contribution of O element from O_2, the quantification of the XPS peaks gives an average Sb:O atomic ratio of 1.000:1.620, which is close to the atom ration from chemical calculation within the range of experimental errors.

The representative FE-SEM images of the as-prepared products are shown in Fig. 3, which reveal the as-prepared products consist of a large quantity of micro-sized Sb_2O_3 octahedra. Fig. 3a displays the panoramic FE-SEM image of micro-metered Sb_2O_3 octahedra, and

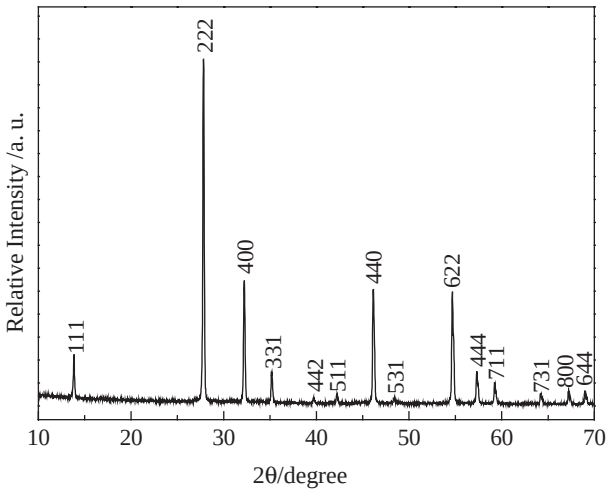

Fig. 1. A typical XRD pattern of the synthetic Sb_2O_3 powders obtained in the presence of PEG-1000 polymers.

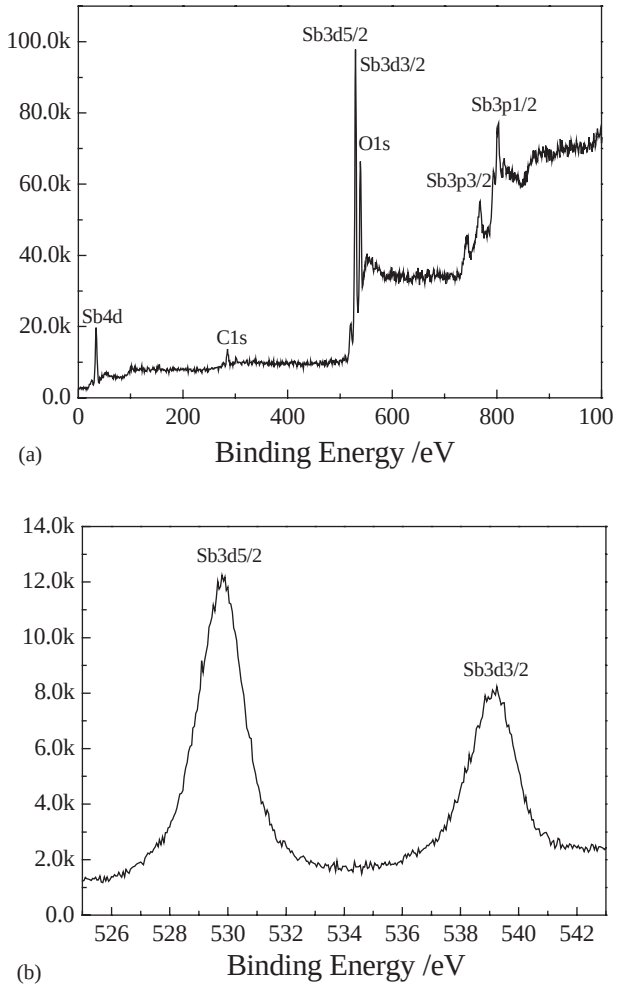

Fig. 2. XPS spectra of micro-sized Sb_2O_3 octahedra: (a) a typical survey spectrum of Sb_2O_3; (b) close-up surveys spectrum for Sb 3*d* core.

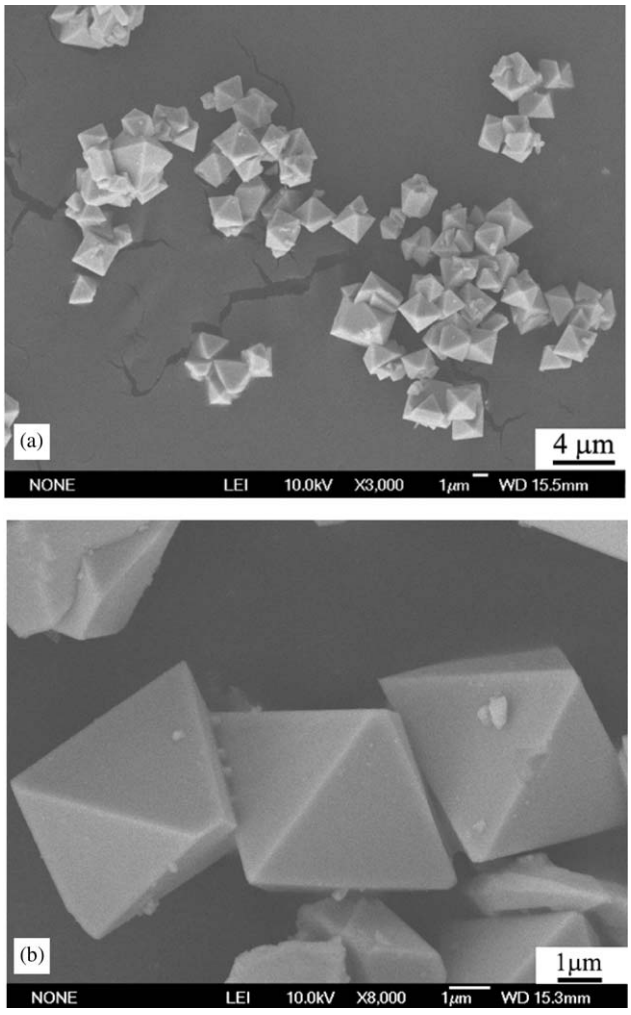

Fig. 3. (a) FE-SEM image of micro-metered Sb_2O_3 octahedra with rather uniform size; (b) a higher-magnification FE-SEM image exhibiting some Sb_2O_3 octahedra.

Fig. 3b presents a higher-magnification FE-SEM image of Sb_2O_3 micro-octahedra, revealing that the as-obtained Sb_2O_3 octahedra are with the typical edges in the range of 3–5 μm.

A study of optical properties of micro-sized Sb_2O_3 octahedra is desirable, because it directly links to their potential optoelectronic applications. PL properties of Sb_2O_3 octahedra are measured at room temperature. Fig. 4a shows the excitation spectrum of Sb_2O_3 micro-octahedra with the emission monitored at 600 nm (2.07 eV), where the excitation peak at 400 nm (3.10 eV) can be observed. And Fig. 4b is the photoluminescence emission spectrum of micro-sized Sb_2O_3 octahedra taken at the excitation wavelength of 400 nm (3.10 eV), in which a sharp peak is located at 600 nm (2.07 eV). To provide additional information on the optical properties of Sb_2O_3 micro-octahedra, Raman scattering technique is used to investigate the vibrational properties of the molecules because it has been proved to be a valuable tool for probing photon excitation in

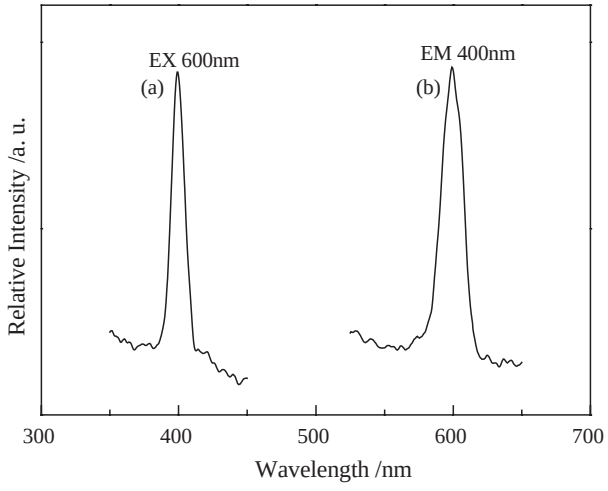

Fig. 4. (a) Photoluminescence excitation spectrum of the micro-sized Sb_2O_3 octahedra with the emission at 600 nm; (b) photoluminescence emission spectrum of Sb_2O_3 micro-octahedra taken at the excitation wavelength of 400 nm.

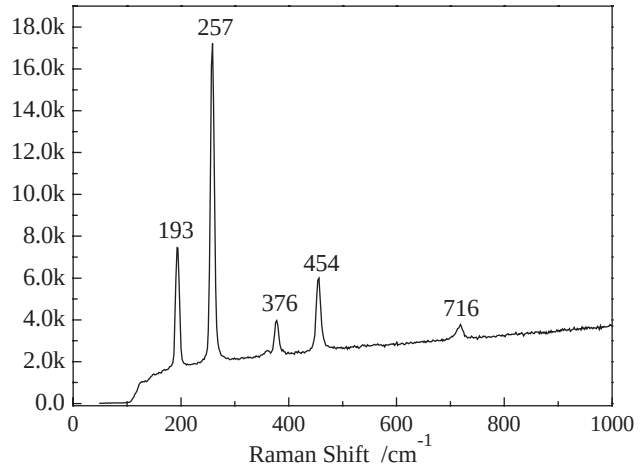

Fig. 5. Raman spectrum of the micro-sized Sb_2O_3 octahedra.

semiconductors. Fig. 5 shows the Raman spectrum of Sb_2O_3 micro-octahedra, which is composed of several optical phonon modes and a broad photoluminescence background. The photon peaks were fitted using seven Lorentzian and one Fano profiles. Additionally, the broad luminescence background was also fitted into a polynomial and subtracted out from the spectrum. From the results shown in Fig. 5, five strong peaks correspond to Raman shifts of 193, 257, 376, 454, and 716 cm^{-1}, respectively, which are in good agreement with the report data [19].

3.2. Results and discussion

The possible chemical reactions for the formation of Sb_2O_3 can be expressed as the following steps: Firstly, Sb^{3+} combines with sodium tartrate to produce Sb(III)(tart.) complex. Secondly, Sb(III)(tart.) complex can react with sodium hydroxide to produce Sb_2O_3. The chemical reaction involved here can be formulated as follows:

$$Sb^{3+} + \text{tart.} \Leftrightarrow \text{Sb(III)(trat.)}, \quad (1)$$

$$2\text{Sb(III)(trat.)} + 6OH^- \rightarrow Sb_2O_3 \downarrow + 2\text{tart.} + 3H_2O. \quad (2)$$

The use of sodium tartrate as a coordination agent is necessary in our experiment, because sodium tartrate can coordinate with Sb^{3+} and avoid producing the precipitation of SbOCl, which can make the system homogeneous. In addition, due to its coordinative effect, sodium tartrate not only can kinetically control the reaction rates but also may provide the octahedral chemical environments for Sb^{3+} ions.

Meanwhile, PEG-1000 plays an important role in the appearance of micro-sized Sb_2O_3 octahedra. PEG-1000 polymer can show considerably high chain flexibility, due to the facilitating of rotation about C–O bonds. The formation of stable complexes results from both the

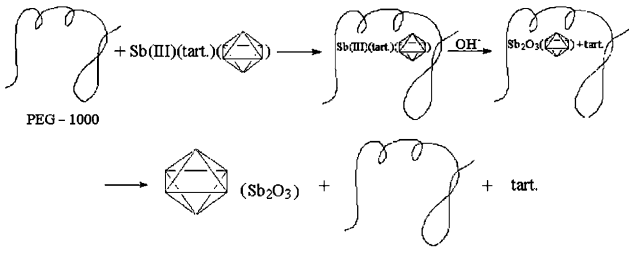

Scheme 1. Illustration of the possible transformation process in the presence of PEG-1000 polymer and sodium tartrate.

increased flexibility of polymer chains and the donor ability of oxygen atoms in PEG polymer [20]. As to our present system, when the amount of PEG-1000 is sufficient, the chains of PEG-1000 may curl around Sb(III)(tart.) and restrict Sb(III)(tart.) in a local region, where Sb(III)(tart.) can react with sodium hydroxide to produce Sb_2O_3. The transformation process can be succinctly illustrated in Scheme 1. Under the influence of the octahedral coordination environment provided by tartrate ions, the renascent Sb_2O_3 nuclei are limited to epitaxial microenvironment and naturally prefer to grow into the octahedra. On the other hand, the reactions proceed in the solution system and the solution approach favors the full expose of the facet of crystal. So, if the capping agent PEG-1000 does not present in the reaction system, the obtained Sb_2O_3 nuclei will grow randomly into the irregular shape. After PEG-1000 is introduced, it is believed that the selective interaction between PEG-1000 and various crystallographic planes of Sb_2O_3 could greatly reduce the growth rate along the $\langle 111 \rangle$ direction and enhance the growth rate along the $\langle 100 \rangle$ direction, which is similar to the reported result [21]. If the concentration of PEG-1000 polymer is too low, the renascent Sb_2O_3 crystals are not effectively capped, and the crystals only exhibit the irregular shapes. With increasing the amount of polymer till to adequately cap the surface of Sb_2O_3, the Sb_2O_3 octahedra with uniform size are obtained. Therefore, under the corporate influence of the above-mentioned factors, the most stable (111) faces preferentially appear and the perfect Sb_2O_3 octahedra are successfully formed. In the supplementary experiments, the procedure is similar except that PEG-1000 is substituted with other PEG polymers with different molecular weight, and a series of SEM observations (Fig. 6b–d) of the products are obtained. For better comparison, the representative SEM image of the as-prepared perfect Sb_2O_3 octahedra is also presented in Fig. 6a. Our previous work [22] has demonstrated that PEG polymers with lower molecular weight (i.e., PEG-200 or PEG-400) are easy to exhibit the full extension of their chain under a certain condition, which is advantageous to the one-dimensional growth, such as microwires and microbrooms (Fig. 6b and c). However, from Fig. 6c, it

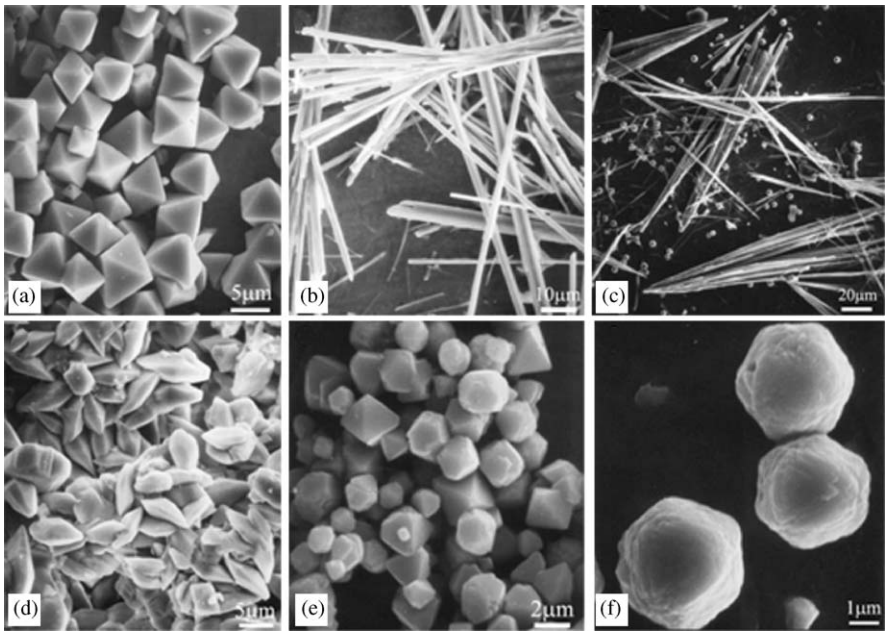

Fig. 6. (a) The representative SEM image of micro-metered Sb_2O_3 octahedra obtained in the presence of PEG-1000; (b) SEM image of Sb_2O_3 microwires with using PEG-200; (c) SEM image of Sb_2O_3 microbrooms involved in PEG-400, showing the coexistence of some irregular-shaped polyhedrons; (d) SEM image of micro-metered Sb_2O_3 rhombis with the use of PEG-2000; (e) SEM image of imperfect Sb_2O_3 micro-octahedra obtained with the temperature lower than 160 °C (also using PEG-1000); and (f) SEM image of imperfect micro-sized Sb_2O_3 octahedra prepared with the reaction time less than 10 h (also involved in PEG-1000).

can also be found that a little amount of irregular-shaped polyhedrons coexist with a mass of micro-brooms, which gives us the inspiration that it is possible to build the regular-shaped polyhedrons when using PEG polymers with appropriate molecular weight. And the perfect micro-sized Sb_2O_3 octahedra have been successfully prepared under the assistance of PEG-1000 polymers, as shown in Fig. 6a. While using the PEG polymer with a larger molecular weight (i.e., PEG-2000), PEG polymers are easier to tangle with each other heavily, which makes the curl effect much stronger than the octahedral coordination effect coming from the Sb(III)(tart.), and the rhombic rather than octahedral morphology would appear (Fig. 6d). Additionally, when utilizing PEG polymers with much larger molecular weight (i.e., PEG-6000), it would be in favor of the formation of three-dimensional architectures, which has been proved in our previous work [23].

Furthermore, the pH value, the reaction temperature and the reaction time have also played key roles in the formation and the morphologies of the products. If the pH value is lower than 8, Sb(III)(tart.) complex is difficult to react with sodium hydroxide and no Sb_2O_3 products can be formed, which may be caused by the much stronger coordination effect of tartrate ions. And only when the pH value is not less than 8.5, Sb_2O_3 products could be obtained. When the reaction temperature is lower than 160 °C or the reaction time is less than 10 h, the products are only imperfect micro-sized Sb_2O_3 octahedra, as shown in Fig. 6e and f, respectively.

4. Conclusions

In summary, the micro-sized Sb_2O_3 octahedra have been successfully synthesized via a simple PEG-1000 polymer-assisted hydrothermal route (PAHR) at 160–180 °C for 10–14 h. The yield of Sb_2O_3 micro-octahedra is as high as ~90%. This is a successful example of the preparation of the micro-metered Sb_2O_3 octahedra via hydrothermal method. On the basis of a series of the supplementary experiments, the possible formation mechanism has been discussed. Since the experimental conditions are controllable, this approach is expected to prepare other octahedral-shaped materials.

Acknowledgments

The financial support from the National Natural Science Research Foundation of China is gratefully acknowledged.

References

[1] T.S. Ma, in: F.J. Welcher (Ed.), Standard Methods of Chemical Analysis, sixth ed., vol. II, Van Nostrand, Princeton, NJ, 1963, p. 357.
[2] T.S. Ma, V. Horak, Microscale Manipulations in Chemistry, Wiley, New York, 1976.
[3] H.M. EI-badry, Micromanipulators and Micromanupulation, Springer, New York, 1963.

[4] S.R. Nicewarner-Pena, R.G. Freeman, B.D. Reiss, L. He, D.J. Pena, I.D. Watton, R. Cromer, C.D. Keating, M.J. Natan, Science 294 (2001) 137.
[5] S. Matthias, J. Schilling, K. Nielsch, F. Müller, R.B. Wehrspohn, U. Gösele, Adv. Mater. 14 (2002) 1618.
[6] Y.W. Jun, Y.Y. Jung, J.W. Cheon, J. Am. Chem. Soc. 124 (2002) 615.
[7] D.J. Dzimitrowice, J.B. Goodenough, P.J. Wiseman, Mater. Res. Bull. 17 (1982) 971.
[8] K. Ozawa, Y. Sakka, A. Amamo, J. Mater. Res. 13 (1998) 830.
[9] D.J. Stewart, O. Knop, C. Ayasse, F.W.D. Woodhams, Can. J. Chem. 50 (1972) 690.
[10] Y.P. Liu, Y.H. Zhang, M.W. Zhang, W.H. Zhang, Y.T. Qian, L. Yang, C.S. Wang, Z.W. Chen, Mater. Sci. Eng. B 49 (1997) 42.
[11] Z.L. Zhang, L. Guo, W.D. Wang, J. Mater. Res. 16 (2001) 803.
[12] Z.L. Zhang, J. Mater. Res. 17 (2002) 1698.
[13] L. Guo, Z.H. Wu, T. Liu, W.D. Wang, H.S. Zhu, Chem. Phys. Lett. 318 (2000) 49.
[14] D.W. Zeng, C.S. Xie, B.L. Zhu, W.L. Song, Mater. Lett. 58 (2004) 312.
[15] C.H. Ye, G.W. Meng, L.D. Zhang, G.Z. Wang, Y.H. Wang, Chem. Phys. Lett. 363 (2002) 34.
[16] Y.X. Zhang, G.H. Li, L.D. Zhang, Chem. Lett. 33 (2004) 334.
[17] S. Friedrichs, R.R. Meyer, J. Sloan, A.I. Kirkland, J.L. Hutchison, M.L.H. Green, Chem. Commun. (2001) 929.
[18] U.A. Schubert, F. Anderle, J. Spengler, J. Zuehlker, H.J. Eberle, R.K. Grasselli, H. Knoezinger, Top. Catal. 15 (2001) 195.
[19] I.A. Degen, G.A. Newman, Spectrochim. Acta 49A (1993) 859.
[20] F. Ciardelli, E. Tsuchida, D. Wöhrle, Macromolecule–Metal Complexes, Springer, Berlin, 1996.
[21] X. Zhang, Y. Xie, F. Xu, X.H. Liu, D. Xu, Inorg. Chem. Commun. 7 (2004) 192.
[22] X.C. Ma, Z.D. Zhang, X. Wang, S.T. Wang, F. Xu, Y.T. Qian, J. Cryst. Growth 263 (2004) 491.
[23] F. Xu, Y. Xie, X. Zhang, C.Z. Wu, W. Xi, J. Hong, X.B. Tian, N. J. Chem. 27 (2003) 1331.